THE ASTROPHYSICAL JOURNAL, 460:1027–1033, 1996 April 1

DOPPLER MEASUREMENTS OF THE SUN'S MERIDIONAL FLOW

DAVID H. HATHAWAY
Mail Code ES82, NASA/Marshall Space Flight Center, Huntsville, AL 35812
Received 1995 August 11; accepted 1995 October 4

ABSTRACT

Doppler velocity data obtained with the Global Oscillation Network Group (GONG) instruments in Tucson from 1992 August through 1995 April were analyzed to determine the structure and evolution of the Sun's meridional flow. Individual measurements of the flow were derived from line-of-sight velocity images averaged over 17 minutes to remove the *p*-mode oscillation signal. Typical flow velocities are poleward at ~ 20 m s^{-1}, but the results suggest that episodes may occur with much stronger flows. Such variations may help to explain some of the many disparate reports on the strength and structure of the Sun's meridional flow.

Subject headings: hydrodynamics — Sun: activity — Sun: interior — Sun: oscillations

1. INTRODUCTION

Meridional circulations can play important roles in the dynamics of stellar convection zones. As these axisymmetric flows carry mass from one latitude to another they also transport heat, angular momentum, and magnetic fields. Models for the dynamics of rotating convection zones usually either include or produce meridional circulations, but the nature of the meridional flow often depends upon the model. Three-dimensional hydrodynamical models, such as those of Glatzmaier & Gilman (1982), tend to produce meridional flows directed from the equator toward the poles in the surface layers. Axisymmetric models, such as those of Belvedere & Paternò (1976), tend to have equatorward meridional flows at the surface. Snodgrass & Wilson (1987) have suggested, on observational grounds, that multicellular circulation patterns that propagate toward the equator might be present on the Sun, and Durney (1993) has produced theoretical arguments that also suggest a multicellular component. Reliable observations of the Sun's meridional flow would help to constrain some of these theories and provide a better understanding of the solar dynamo mechanism in particular and stellar convection zone dynamics in general.

Unfortunately, previous measurements of the Sun's meridional circulation have produced a bewildering array of results that appear to be of no help at all in constraining theory. Some investigators report poleward flows while others find equatorward flows. Most investigators find weak flows on the order of 10–20 m s^{-1} while others find flows an order of magnitude stronger. Some authors suggest that there may be variations in the flows associated with the solar cycle while others find more chaotic behavior or no variations at all. The primary reason for this lack of consensus is the relative weakness of the flow itself and the difficulty associated with separating the meridional flow signal from other signals. These other signals include those of solar origin, such as the 2000 m s^{-1} rotation signal and the 100 m s^{-1} convective limb shift signal caused by the correlations between velocity and intensity in the unresolved convective elements. Signals of instrumental origin, such as spectrograph noise in the Doppler measurements, are also sources of error. Recently, new analysis techniques have been developed that cleanly separate the various solar Doppler velocity signals (Hathaway 1987, 1992a). In addition, new instruments, such as those developed by the Global Oscillation Network Group (GONG), are now providing greatly improved Doppler velocity data. This combination now allows for more accurate determinations of the meridional flow velocity and studies of temporal changes in its strength and structure.

2. PREVIOUS RESULTS

Two principal methods are used to measure the meridional flow: feature tracking and direct Doppler measurement. Feature tracking involves identifying and tracking solar features such as sunspots, filaments, or magnetic elements. Doppler measurements involve measuring the Doppler shift of spectral lines formed in the solar photosphere. Both techniques yield a wide range of results for the meridional flow.

Feature tracking usually yields a poleward meridional flow of ~ 10 m s^{-1}. Such flows were found by Topka et al. (1982) using polar filaments; by Howard & Gilman (1986) using sunspots; by Wang, Nash, & Sheeley (1989) using magnetic field patterns; by Howard (1991) using active region magnetic fields; by Komm, Howard, & Harvey (1993) using small magnetic features; and by Latushko (1994) also using magnetic features. In contrast, Ribes, Mein, & Mangeney (1985) found alternating flows of up to 100 m s^{-1} using sunspots, and Kambry et al. (1991) found a 10 m s^{-1} equatorward flow using sunspots.

There are several problems associated with using tracers to measure surface velocities such as the meridional flow. Sunspots and filaments do not provide the best spatial or temporal coverage for such studies. Sunspots are limited to low latitudes and are difficult to find near sunspot cycle minima. Filaments provide somewhat greater coverage, but their morphology often makes it difficult to accurately locate a distinct feature. A fundamental problem with all tracers is the uncertainty about what level of the atmosphere or interior their motions represent.

Doppler velocity measurements provide another means of measuring the meridional flow. While these measurements do not suffer from some of the problems associated with feature tracking, they do include additional signals and sources of error. The most difficult problem is separating the meridional flow from the convective limb shift signal. The convective limb shift is a variation in the Doppler velocity from the disk center to the limb. It is produced by the correlation of intensity with velocity in the unresolved

granulation (Beckers & Nelson 1978). It appears as a blueshift at disk center that decreases in amplitude away from the center and may even become a redshift close to the limb. The manner in which the limb shift varies is a function of the spectral line used for the measurements. Some spectral lines show a monotonic variation from disk center to limb while others exhibit an increasing blueshift followed by the usual decrease.

The analyses of Doppler velocity data generally fall into two categories: (1) comparing velocity scans from disk center to the east and west limbs with scans from disk center to the north and south limbs and (2) fitting the velocity pattern over the solar disk with various functions representing the different signals. With the east-west versus north-south method, the solar rotation signal is removed by averaging velocities from either side of disk center in an east-west direction. This signal contains the limb shift velocity but not the meridional flow, since it is directed transverse to the line of sight. The north-south scan contains both of these signals. The difference between the north-south and east-west scans then provides a measure of the meridional flow. With the fitting method, functions are taken to represent the various velocity signals, and a least-squares fit is found to determine the amplitudes of these functions.

The east-west versus north-south method was first used by Duvall (1979), who found a poleward flow of ~ 20 m s^{-1}. Andersen (1984) used this technique and found a poleward flow of ~ 50 m s^{-1} near the equator but with an equatorward flow of ~ 80 m s^{-1} poleward of 45°. In a later paper, Andersen (1987) found a poleward flow of 20–25 m s^{-1}. Ulrich et al. (1988) also found an average poleward flow of ~ 20 m s^{-1} but with variations from more than 70 m s^{-1} poleward to nearly 40 m s^{-1} equatorward.

Cavallini, Ceppatelli, & Righini (1985) performed a detailed study of the changes in spectral line shape from disk center to limb along the east-west and north-south directions. They measured the positions of the bisectors of three spectral lines at different intensity levels and found that the shapes of the lines had similar variations along each scan direction, but with different shifts in the line positions. Although this would suggest that the line shifts were true Doppler shifts, they cautioned against this interpretation because they found slightly different shifts for the different lines. In a later paper (Cavallini, Ceppatelli, & Righini 1986) they extended their analysis to two more lines and again found that the line shapes are functions of center-to-limb distance only. In this paper they inferred a poleward flow of 50–70 m s^{-1}. However, after noting the many different results from other investigators they concluded that the signal might be due to a latitudinal variation in the convective elements that contribute to the limb shift signal.

Using fitting methods, Beckers (1978) found a poleward flow of ~ 40 m s^{-1}, while Howard (1979) found a poleward flow of ~ 20 m s^{-1} and Pérez Garde et al. (1981) found an equatorward flow of ~ 20 m s^{-1}. LaBonte & Howard (1982) revised the fitting procedure but still found a poleward flow of ~ 20 m s^{-1}. Snodgrass (1984) then used a new set of functions and found a slightly weaker poleward flow of ~ 10 m s^{-1}.

These two methods of analyzing Doppler velocity data have their own advantages and disadvantages. The east-west versus north-south method does a good job of cleanly separating the limb shift and meridional flow signals. However, it uses data only from a small part of the visible disk, so the results tend to be noisy and require many days of data to obtain a good measurement. The fitting techniques use data from the entire disk and could be less noisy but they have not cleanly separated the limb shift and the meridional flow signals.

Given the array of results from all of these methods, it has been difficult to reach any conclusions about the Sun's meridional flow. While most studies indicate a fairly weak flow of 10–20 m s^{-1}, many found flows much stronger than this, some found flows directed in opposite directions, and some questioned the source of the signal itself. Resolving these problems requires better data and better data analysis techniques that can reliably extract the meridional flow signal without the large scatter seen in previous studies. The following sections describe new data and analysis techniques that meet these requirements. The most recent results indicate that the meridional flow is poleward at ~ 20 m s^{-1}, but earlier data suggest that the meridional flow may vary in time with the usually weak flow punctuated by episodes with much stronger flow.

3. OBSERVATIONS

The GONG has developed a set of instruments to measure the line-of-sight Doppler velocity over the surface of the Sun at 60 s intervals (Harvey et al. 1988). Six of these instruments have been deployed at a network of sites around the world to provide nearly continuous observations of the global oscillations of the Sun. A prototype instrument has been in use at a site in Tucson since 1992 August, and the field instruments became operational in 1995.

The data consist of images obtained at three phases of one Fourier component of the Ni I 676.8 nm absorption line on a 256 × 242 pixel CCD. These images are combined to produce an intensity image, a line-of-sight velocity image, and a modulation image (which shows variation in the equivalent width of the line). Images are obtained at a 60 s cadence and then averaged over 17 minutes with a Gaussian-shaped weighting function to remove the global oscillation signal due to p-modes with periods of ~ 5 minutes. A series of these images were acquired from the GONG project by requesting all such data obtained at 20:00 UT on days from 1992 August through 1995 April. This included data from the prototype instrument, tc, and from four of the "farm" instruments, fb, fd, fe, and ff. In all, over 200 days are represented, with simultaneous data from two instruments on 45 days between 1994 October and 1995 April. The 202 days are nonuniformly distributed over the 34 months and have increasingly better coverage toward the end of this period.

4. ANALYSIS

The velocity images were analyzed using a technique developed previously by the author (Hathaway 1987, 1992a). The intensity images are used to determine the position, size, shape, and orientation of the solar images. The solar ephemerides are referred to for the position angle and tilt of the Sun's rotation axis. The velocity signal due to the Sun-observer relative motion is then removed from the data in a preliminary step.

The most difficult part of the analysis is to cleanly separate the meridional flow signal from the convective

limb shift signal. Many of the earlier analyses used a power law to represent the limb shift with

$$V_{\rm LS}(\rho) = \alpha(1 - \cos\rho)^{\beta}\,, \tag{1}$$

where α is a constant, ρ is the heliocentric angle from disk center, and β is a constant (usually ~ 3). For many spectral lines the blueshift may first increase before decreasing away from disk center. Bruning (1981) showed that for these lines a polynomial in $(1 - \cos\rho)$ is a much better representation. Here the limb shift is determined by first finding the average velocity in 256 annular rings about disk center with equal spacing in $(1 - \cos\rho)$. The average radial position of the points in each ring is determined, and then this signal is fitted to a third-order polynomial such that

$$V_{\rm LS}(\rho) = \sum_{n=0}^{3} C_n(2n+1)^{-1/2}P_n^*(1 - \cos\rho)\,, \tag{2}$$

where the values of C_n are amplitude coefficients for the components of the limb shift and the values of P_n^* are the shifted Legendre polynomials (see Appendix). (Earlier analyses included the fourth-order polynomial, but the results indicated that the signal was well represented without this component.) This polynomial fit is removed from the data before proceeding to the meridional flow analysis step. The rotation signal does not contribute to the average signal in any ring because of its change in sign on either side of the central meridian. The meridional flow, however, will contribute to this average, so the coefficients from this preliminary limb shift determination must be corrected for the presence of any meridional flow. These corrections are easily determined and accounted for after the meridional flow signal is determined.

The meridional flow signal is found by fitting the remaining Doppler velocity signal to a polynomial form for the meridional flow. The axisymmetric meridional flow is represented by spherical harmonics with

$$U_{\rm MF}(\theta) = -\sum_{l} S_l^0 P_l^1(\cos\theta)\,, \tag{3}$$

where $U_{\rm MF}$ is the meridional flow velocity toward the south pole on the solar surface, θ is the polar angle from the north pole, the values of S_l^0 are spectral coefficients that characterize the axisymmetric meridional flow, and the values of P_l^1 are the normalized associated Legendre polynomials of degree l and order $m = 1$ (see Appendix and Hathaway 1992a for details). The degree, l, of each component gives the number of circulation cells between the poles. The observed line-of-sight velocity produced by this flow is given by

$$V_{\rm MF}(\theta, \phi) = -\sum_{l} S_l^0 F_l(B_0, \theta, \phi)\,, \tag{4}$$

where ϕ is the azimuthal angle (longitude) from the central meridian, B_0 is the latitude at disk center (the tilt of the Sun's rotation axis toward the observer), and

$$F_l(B_0, \theta, \phi) = P_l^1(\cos\theta)(\sin B_0 \sin\theta - \cos B_0 \cos\theta \cos\phi)\,. \tag{5}$$

The important point to note here is that this signal is altered by the removal of a third-order polynomial fit to its average around concentric rings during the limb shift analysis step. The polynomial fit to this signal is given by

$$\bar{V}_{\rm MF}(\rho) = -\sum_{l} S_l^0 \bar{F}_l(B_0, \rho)\,, \tag{6}$$

with

$$\bar{F}_l(B_0, \rho) = \left(\frac{2}{2l+1}\right)^{1/2} P_l^0(\sin B_0) \sum_{n=0}^{3} \chi_l^n P_n^*(1 - \cos\rho)\,, \tag{7}$$

where the values of P_l^0 are the associated Legendre polynomials of order $m = 0$ and the the values of χ_l^n are cross-talk coefficients given by

$$\chi_l^n = \int_0^1 \sin\rho P_l^1(\cos\rho)P_n^*(x)dx\,, \tag{8}$$

with $x = 1 - \cos\rho$ (see Appendix for evaluated coefficients). The resulting functional form for the meridional flow signal after the preliminary limb shift has been removed is then

$$V_{\rm MF}(\theta, \phi) = -\sum_{l} S_l^0\{F_l(B_0, \theta, \phi) - \bar{F}_l[B_0, \rho(\theta, \phi)]\}\,. \tag{9}$$

The spectral coefficients, S_l^0, for $l = \{1, 8\}$ are determined by a least-squares fit of these functions to the velocity data.

One problem that arose in analyzing these data concerns the presence of active regions. Magnetic fields in active regions alter the granulation pattern and change the limb shift signal. While the nature of these changes should be better understood and accounted for in the future, in the present study the active regions are simply masked out and filled in with a velocity field containing the rotation, limb shift, and meridional circulation signals. This velocity field is determined by an iterative procedure that uses the previously determined spectral coefficients to fill in the masked areas until the analysis produces no further changes in the spectral coefficients. The masks are constructed with magnetograms reproduced from the NSO/Kitt Peak synoptic magnetic field maps. The magnetic maps were differentially rotated so that the central meridian matches the time of observation. The maps are then projected onto the solar disk with the appropriate position angle and tilt of the Sun's rotation axis. All pixels with field strengths above some cutoff value are masked out along with the eight surrounding pixels.

Another problem that arose in analyzing the earlier data concerns determining the position angle of the Sun's rotation axis. Although the GONG project tried to place the Sun's rotation axis along pixel columns of the detector, errors were introduced as the adjustments were made to the instruments. An error of 1° in the position angle produces a north-south velocity gradient with a difference of 35 m s^{-1} between disk center and the polar limb positions. This appears as a signal in the odd l meridional flow coefficients with most of it contained in the S_1^0 term. Procedural changes were made in 1994 October that eliminated these errors. When the GONG instruments were placed at their permanent sites, this new procedure was also used. For the present analysis, however, the errors are removed by choosing the rotation axis position angle that gives $S_1^0 = 0$. Although this precludes using any information from this term and also makes the other odd l terms uncertain, it gives a cleaner analysis, as evidenced by the smaller residual velocities that it produces. Prior to 1994 October the variations in the position angle were as large as $\pm 2°$. After this period the variations were less than $\pm 0°.25$.

5. RESULTS

The 202 daily images from 1992 August through 1995 April were analyzed using the technique described in the previous section. The active region masks were constructed from the NSO/Kitt Peak synoptic maps by masking out all pixels with magnetic intensities greater than 50 G. Comparing the structure of these masks with the structures visible in the modulation images provided assurance that active region structures were effectively removed by the masks. The results of the analysis for the meridional flow component with two cells, one in each hemisphere, are shown in Figure 1. Positive values for the amplitude indicate flows directed from the equator toward the poles in both hemispheres. The flow velocity appears to increase from ~ 20 m s^{-1} in the summer of 1992 to more than 80 m s^{-1} in mid to late 1993. It then decreased to ~ 10 m s^{-1} in the summer of 1994 and then slowly increased to ~ 25 m s^{-1} by the end of April of 1995.

During the 1993 period when the flow velocity was large, the variance also increased, but not in a manner that suggests larger random variations. During the May–June time period there were observations nearly every day, and the meridional flow signal varied almost sinusoidally from 70 m s^{-1} down to 30 m s^{-1}, up to 80 m s^{-1}, and then back down to ~ 50 m s^{-1}. Later that year, from September through December, the flow increased monotonically from ~ 20 m s^{-1} up to ~ 80 m s^{-1}. One source of these variations might be large-scale nonaxisymmetric flows that would contribute directly to the Doppler signal and vary as the Sun's monthly rotation carries them through the field of view.

The results for the meridional flow component with four cells, two in each hemisphere, are shown in Figure 2. Positive amplitudes indicate flows that diverge in the midlatitudes and converge at the equator and poles. The amplitude is largely positive with an average of ~ 5 m s^{-1} from mid 1992 until the end of 1993. The amplitude then drops to an average closer to zero in 1994 and 1995. Results with earlier data (Hathaway 1992b, 1993) indicated a negative value for this component, in agreement with the observations of Komm et al. (1993) and the theoretical arguments of Durney (1993). This suggests that this component may change direction from time to time. All of the odd components—those with flows that cross the equator, as well as the higher order even components—show amplitudes with a small (< 5 m s^{-1}) scatter about zero amplitude.

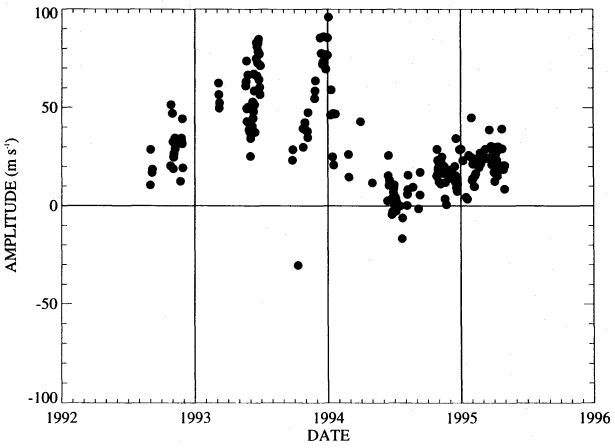

FIG. 1.—History of the $l = 2$ component from 1992 August through 1995 April. Positive values indicate flows directed from the equator toward the pole in both hemispheres. The flow velocity increases from ~ 20 m s^{-1} in the summer of 1992 to more than 80 m s^{-1} in mid to late 1993. It then decreases to nearly zero in the summer of 1994 before returning to a fairly steady level of ~ 20 m s^{-1} in the first half of 1995.

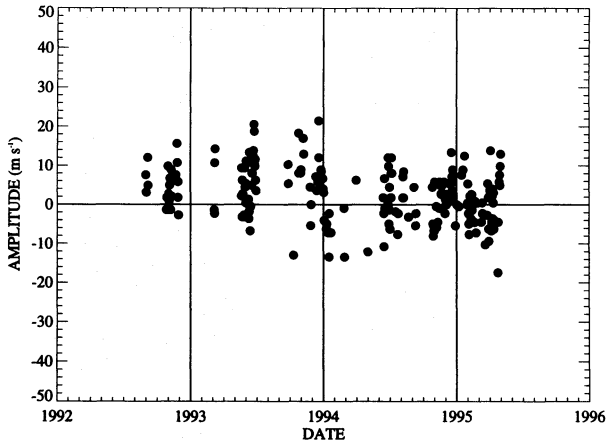

FIG. 2.—History of the $l = 4$ component from 1992 August to 1995 April. Positive values indicate flows that diverge from the midlatitudes and converge at the equator and the poles. Small positive values with amplitudes of ~ 5 m s^{-1} are found from mid 1992 until the end of 1993. This component then drops to near zero after the start of 1994.

Figure 3 shows the meridional flow profiles constructed from 6 month averages of the meridional flow coefficients. The peak flow velocity was nearly 40 m s^{-1} in late 1992. The flow speed increased to nearly 60 m s^{-1} throughout 1993 and then decreased to less than 30 m s^{-1} in 1994 and 1995. Although the S_1^0 component has been forced to zero, the other odd components do contribute to produce some north-south asymmetries in these profiles. The extreme limb is excluded in this analysis, so flow velocities poleward of $\sim 75°$ are extrapolations from the lower latitudes.

The meridional flow velocities in 1993 were much higher than expected. Several tests were performed with this data to confirm these results. The daily velocity images for 1993 May and June were averaged together to produce an image with good statistics for the north-south versus east-west velocity scan analysis method. Data from a scan along the equator were folded about disk center and averaged. Similar data from a scan along the central meridian were also folded and averaged. The east-west scan contains the limb shift signal without the signal due to meridional flow.

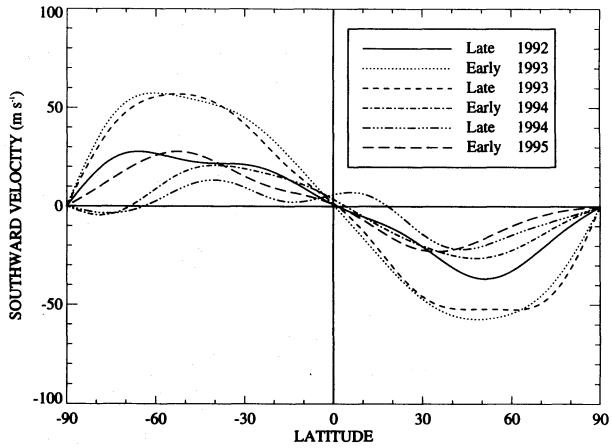

FIG. 3.—Meridional flow profiles for 6 month intervals. The meridional flow velocities (positive toward the south pole) are plotted as functions of latitude for six 6 month intervals from late 1992 to early 1995. Flow speeds throughout 1993 were nearly twice as strong as flow speeds at other times.

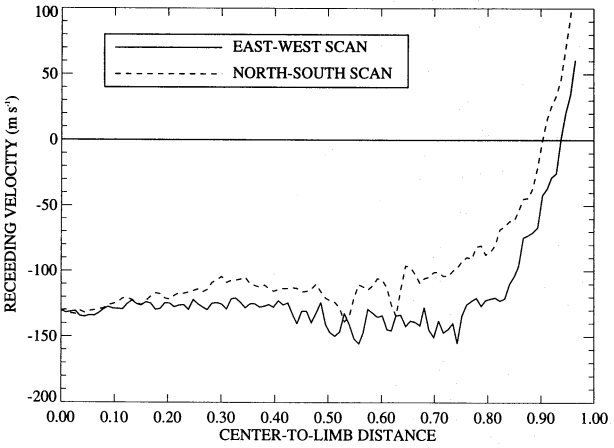

FIG. 4.—East-west and north-south velocity scans for 1993 May and June. The velocity signal along an east-west scan averaged on either side of disk center is shown as a function of the distance from disk center with the solid line. The velocity signal along a north-south scan averaged on either side of disk center is shown with the dashed line. The difference between the two indicates a meridional flow of ~ 60 m s^{-1}.

The north-south scan contains both the limb shift and the meridional flow signals. These velocity scans are shown in Figure 4. The velocities along the central meridian are redshifted relative to those along the equator. The velocity difference at 70% of the distance from disk center to limb is ~ 40 m s^{-1}. This indicates a meridional flow of ~ 60 m s^{-1}, which is in good agreement with the average of S_2^0 for this time period as seen in Figures 1 and 3. This agreement indicates that the signal is in the data and is not an artifact or error in the analysis procedures.

Another possible source of the meridional flow signal is inadequate masking of the active regions during this period of time. The active region masks might be too small, or they might be misplaced by errors in the image size, position, or orientation. The position angle used for the Sun's rotation axis ranged from $-1°$ to $+2°$ from the nominal position given by the GONG project. This image rotation might move the velocity image with respect to the mask and expose active region areas that were meant to be covered. The data analysis was repeated using the GONG position angles to test this possibility. The differences in the results were minor, less than 1 m s^{-1} for angles up to $\pm 1°$ and less than ~ 2 m s^{-1} at the larger angles. This shows that the results, for the even components at least, are relatively insensitive to errors in the position angle.

A further test of the masking was performed by comparing results with different masking criteria. Changing the cutoff value in the magnetic intensity from 50 G up to 100 G and down to 25 G typically changes the masked area from 5% down to 3% and up to 10% during the 1993 May and June time period. The results of the analyses with these different masks were virtually identical. The S_2^0 component varied by less than 2 m s^{-1}. These two tests indicate that the meridional flow signal is not a product of the "spurious" velocity signals in active regions or changes in masked areas.

Yet another possible source of the meridional flow signal is the cross talk with the limb shift signal. Although considerable effort has gone into removing the cross talk within the present analysis procedures, this has been a problem with previous analyses. If the meridional flow signal is tied to the limb shift signal, we might expect to see similar variations in the limb shift. Figure 5 shows the history of the limb

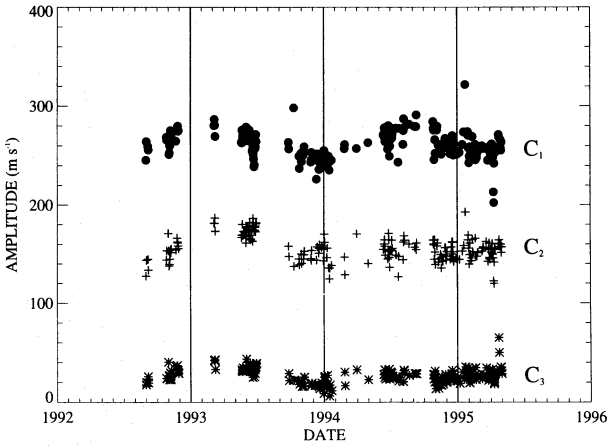

FIG. 5.—History of the limb shift components from 1992 August through 1995 April. The amplitudes, C_n, of the limb shift components are fairly constant. The total variation for the signal is only ~ 10 m s^{-1}, with little correlation to the changes in the meridional flow.

shift components. The amplitudes of the components are fairly constant. The total variation of the signal is only ~ 10 m s^{-1}, with little correlation to the changes in the meridional flow.

A final test of these results is to compare simultaneous measurements from different instruments. Unfortunately, the GONG instruments are the only ones obtaining velocity data in this spectral line, and the additional GONG instruments did not become functional until after 1994 October, a period in which both the signal and its variations were small. Nonetheless, comparing results from these additional instruments is reassuring, as seen in Figure 6. The "farm" instrument fb is represented by the filled circles. Instruments fd, fe, and ff are represented by the pluses, asterisks, and open circles, respectively. The agreement is quite good. In many cases the measurements are virtually identical, and in all cases they have similar scatter about the same mean values. During this time interval the signal increases from ~ 15 m s^{-1} to ~ 25 m s^{-1}.

6. DISCUSSION

The analysis of these observations shows that the Sun's meridional flow can be measured with unprecedented accu-

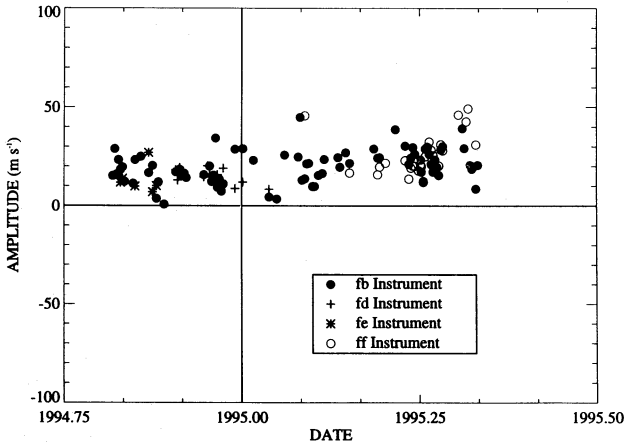

FIG. 6.—Comparison of the S_2^0 component determined from observations with different GONG instruments. The fb instrument results are represented by the filled circles, and the other GONG instruments are represented by asterisks, pluses, and open circles. The agreement between these different instruments is very good, with similar mean values and variations.

racy using this analysis technique with GONG Doppler velocity data. Previous measurements by other groups showed day-to-day scatter nearly an order of magnitude higher than with the present study. The improvement in accuracy reveals possible temporal variations in the strength and structure of the meridional flow. The flow is generally directed from the equator toward the poles, but it may vary in amplitude by a factor of 2 or more on a timescale of months. The flow speed increased from ~ 30 m s^{-1} in late 1992 to nearly 60 m s^{-1} in 1993 and then dropped to ~ 20 m s^{-1} in 1994. High flow speeds were also seen in earlier data, as reported by Hathaway (1992b, 1993). That earlier report generated some cautions from the community, so additional efforts were undertaken here to provide assurances that the results were not in error.

The analysis technique described here and in earlier papers has been tested extensively with artificial data and found to work extremely well. The high flow velocities were confirmed through the use of an older, entirely different technique, the comparison of east-west and north-south velocity scans. In order to use this older technique, the data had to be averaged over more than a month to reduce the contributions from other solar signals such as supergranulation. With the new technique, reliable results can be obtained from a single velocity image obtained over a 17 minute interval.

Tests were undertaken to rule out contributions to this velocity signal from "spurious" velocities in active regions. Active regions are masked out in this analysis, and the results are fairly insensitive to the size of the masked areas. Although there were some problems in accurately determining the position angle of the Sun's rotation axis prior to 1994 October, the results are insensitive to these changes as well. The masked area does change substantially during this declining phase of cycle 22. The masked area drops from $\sim 7\%$ in 1992 to $\sim 1\%$ in 1995, but tests of the sensitivity of this technique to the size of the masked area suggest that this is not a source of the signal or its variation.

Results with different GONG instruments show good agreement. Unfortunately, the larger signals and the large variations all occurred when only one instrument was available and while that instrument was under development. However, the spatial structure of this meridional flow signal is quite unique. It consists of redshifted bands on either side of the equator with the signal tapering off toward both the equator and the limb. It is difficult to believe that instrumental problems would influence this component to such a degree without also changing other components as well. Furthermore, during the period when multiple instruments were available, there were still variations, albeit weaker, in the strength of the signal. Again, this suggests that the results are not of instrumental origin.

Several authors have suggested that the meridional flow signal might be due to a latitude-dependent limb shift. Since the limb shift signal is formed by the correlations between velocity and intensity in the solar granulation pattern, latitudinal variations in the granulation could very well influence the meridional flow signal. The granulation is known to be different in active regions, but the active regions are masked out in the present study, and the results do not depend strongly on the size of these masks. The granulation also changes the shape of the spectral line as measured by the line bisectors, but the shape does not appear to vary with latitude (Cavallini et al. 1985, 1986). One would also expect that if the signal were due to a latitude-dependent limb shift, then the temporal variations in this signal would also be reflected in the limb shift measurements, and they are not. These results suggest that the signal is not due to a latitude-dependent limb shift but results from a meridional flow.

If the meridional flow signal and its variations are truly what they appear to be, a meridional flow in the solar photosphere that varies on a timescale of months, then we can accept many of the previous results as further evidence for temporal variations of this flow. With somewhat less than 3 years of data, it is difficult to determine any solar cycle trends from the current data. The results do suggest, however, that the Sun may undergo episodes in which the meridional flow increases dramatically. Further study is needed to determine the relationship between these variations and other solar processes.

This work was supported by NASA's Space Physics Division through its Solar Physics Branch. This work utilizes data obtained by the Global Oscillation Network Group (GONG) project, managed by the National Solar Observatory, a Division of the National Optical Astronomy Observatories, which is operated by AURA, Inc., under a cooperative agreement with the National Science Foundation. The author would like to thank Jack Harvey, Frank Hill, John Leibacher, Steve Suess, and an anonymous referee for their helpful comments on this paper.

APPENDIX A

The orthonormal functions and the cross-talk coefficients used in this analysis are presented here for reference and completeness. The first eight normalized associated Legendre polynomials of order $m = 1$ are used to represent the meridional velocity. These polynomials are

$$P_1^1(x) = (3/4)^{1/2}(1 - x^2)^{1/2}, \tag{A1}$$

$$P_2^1(x) = (15/4)^{1/2}x(1 - x^2)^{1/2}, \tag{A2}$$

$$P_3^1(x) = (21/32)^{1/2}(5x^2 - 1)(1 - x^2)^{1/2}, \tag{A3}$$

$$P_4^1(x) = (45/32)^{1/2}(7x^3 - 3x)(1 - x^2)^{1/2}, \tag{A4}$$

$$P_5^1(x) = (165/256)^{1/2}(21x^4 - 14x^2 + 1)(1 - x^2)^{1/2}, \tag{A5}$$

$$P_6^1(x) = (273/256)^{1/2}(33x^5 - 30x^3 + 5x)(1 - x^2)^{1/2}, \tag{A6}$$

$$P_7^1(x) = (105/4096)^{1/2}(429x^6 - 495x^4 + 135x^2 - 5)(1 - x^2)^{1/2}, \tag{A7}$$

$$P_8^1(x) = (153/4096)^{1/2}(715x^7 - 1001x^5 + 385x^3 - 35x)(1 - x^2)^{1/2}. \tag{A8}$$

TABLE 1

LIMB SHIFT–MERIDIONAL FLOW CROSS-TALK COEFFICIENTS

	χ_l^n			
l	$n = 0$	$n = 1$	$n = 2$	$n = 3$
1.....	$1/3^{1/2}$	$1/4$	$-1/(4 \times 15^{1/2})$	0
2.....	$15^{1/2}/8$	$-1/(8 \times 5^{1/2})$	$-3^{1/2}/8$	$3^{1/2}/(8 \times 35^{1/2})$
3.....	0	$-7^{1/2}/(4 \times 2^{1/2})$	$-3 \times 3^{1/2}/(4 \times 70^{1/2})$	$3^{1/2}/(8 \times 2^{1/2})$
4.....	$-5^{1/2}/(8 \times 2^{1/2})$	$-15^{1/2}/(8 \times 2^{1/2})$	$5/(16 \times 2^{1/2})$	$17 \times 5^{1/2}/(48 \times 14^{1/2})$
5.....	0	$55^{1/2}/64$	$5 \times 33^{1/2}/64$	0
6.....	$273^{1/2}/128$	$3 \times 91^{1/2}/128$	$3 \times 273^{1/2}/(128 \times 5^{1/2})$	$-7 \times 39^{1/2}/128$
7.....	0	$-3 \times 7^{1/2}/(64 \times 5^{1/2})$	$-3 \times 21^{1/2}/64$	$-91/(64 \times 15^{1/2})$
8.....	$-3 \times 17^{1/2}/128$	$-3 \times 51^{1/2}/128$	$-3 \times 17^{1/2}/(32 \times 5^{1/2})$	0

The first four shifted Legendre polynomials are used to represent the convective limb shift. These polynomials are orthonormal on the interval $x = \{0, 1\}$ with unit weight and are given by

$$P_0^*(x) = 1 , \tag{A9}$$

$$P_1^*(x) = 3^{1/2}(2x - 1) , \tag{A10}$$

$$P_2^*(x) = 5^{1/2}(6x^2 - 6x + 1) , \tag{A11}$$

$$P_3^*(x) = 7^{1/2}(20x^3 - 30x^2 + 12x - 1) . \tag{A12}$$

The cross-talk coefficient matrix gives the mixing between the limb shift and meridional flow signals and is given by Table 1.

REFERENCES

Andersen, B. N. 1984, Sol. Phys., 94, 49
———. 1987, Sol. Phys., 114, 207
Beckers, J. M. 1978, in Proc. Workshop on Solar Rotation, ed. G. Belvedere & L. Paternò (Catania: Univ. of Catania), 166
Beckers, J. M., & Nelson, G. D. 1978, Sol. Phys., 58, 243
Belvedere, G., & Paternò, L. 1976, Sol. Phys., 47, 525
Bruning, D. H. 1981, Sol. Phys., 71, 233
Cavallini, F., Ceppatelli, G., & Righini, A. 1985, A&A, 150, 256
———. 1986, A&A, 163, 219
Durney, B. R. 1993, ApJ, 407, 367
Duvall, T. L., Jr. 1979, Sol. Phys., 63, 3
Glatzmaier, G. A., & Gilman, P. A. 1982, ApJ, 256, 316
Harvey, J., & the GONG Instrument Development Team. 1988, in Proc. Symp. Seismology of the Sun and Sun-like Stars, ed. E. J. Rolfe, ESA SP-286, 203
Hathaway, D. H. 1987, Sol. Phys., 108, 1
———. 1992a, Sol. Phys., 137, 15
———. 1992b, BAAS, 24, 736
———. 1993, in ASP Conf. Ser., Vol. 42, GONG 1992: Seismic Investigation of the Sun and Stars, ed. T. M. Brown (San Francisco: ASP), 265
Howard, R. 1979, ApJ, 228, L45
———. 1991, Sol. Phys., 131, 259
Howard, R., & Gilman, P. A. 1986, ApJ, 307, 389
Kambry, M. A., Nishikawa, J., Sakurai, T., Ichimoto, K., & Hiei, E. 1991, Sol. Phys., 132, 41
Komm, R. W., Howard, R. F., & Harvey, J. W. 1993, Sol. Phys., 147, 207
LaBonte, B. J., & Howard, R. 1982, Sol. Phys., 80, 361
Latushko, S. 1994, Sol. Phys., 149, 231
Péres Garde, M., Vásquez, M., Schwan, H., & Wöhl, H. 1981, A&A, 93, 67
Ribes, E., Mein, P., & Mangeney, A. 1985, Nature, 318, 170
Snodgrass, H. B. 1984, Sol. Phys., 94, 13
Snodgrass, H. B., & Wilson P. R. 1987, Nature, 328, 696
Topka, K., Moore, R., LaBonte, B. J., & Howard, R. 1982, Sol. Phys., 79, 231
Ulrich, R. K., Boyden, J. E., Webster, L., Snodgrass, H. B., Padilla, S. P., Gilman, P., & Shieber, T. 1988, Sol. Phys., 117, 291
Wang, Y.-M., Nash, A. G., & Sheeley, N. R., Jr. 1989, ApJ, 347, 529